Kinetics of Adsorption Competition of Pb-Cu and Pb-Methylene Blue in Aqueous Solution using Silica Gels from Coal Fly Ash

DOI:10.36909/jer.13971

Yudi Aris Sulistiyo[1,*], Vivi Ruthmianingsih[1], Inayatul Mukarromah[1], Tanti Haryati[1], Novita Andarini[1], Suwardiyanto Suwardiyanto[1], Hamza Sani Rabiu[2], Gagus Ketut Sunnardianto[3]

[1]Inorganic Material for Energy and Environmental Research Group, Department of Chemistry, Universitas Jember, Jl. Kalimantan 37, Jember, 68121, East Java, Indonesia.

[2]Department of Applied Chemistry, Federal University Dutsin-ma, Katsina State, Nigeria.

[3]Research Center for Physics, Indonesian Institute of Sciences, Kawasan Puspitek Serpong, Tangerang Selatan, 15314, Banten, Indonesia.

*Email: yudi.fmipa@unej.ac.id; Corresponding Author.

ABSTRACT

The present study investigates the removal of Pb^{2+} using silica gel (SG) in the presence of the Cu^{2+} (Pb-Cu) and methylene blue (Pb-MB) ion competitor. These pollutants are toxic and harmful to the ecosystem. The presence of the multicomponent pollutants causes more complications to remove from the water system. The adsorptions were examined in a batch system under certain experimental conditions (pH solution system and contact time). Meanwhile, the FTIR spectrophotometer determines the differences adsorption interaction in silica functional groups before and after adsorption. The results showed that the silanol group of silica gel acted as an adsorption site. In the single systems, the adsorption capacity of silica gel follows the order MB > Cu^{2+} > Pb^{2+} of around 84.03; 64.81; and 56.88 $mg.L^{-1}$, respectively. The kinetic adsorptions of both single and binary systems were best fitted to pseudo-second-order models. In the binary solution systems, both adsorption capacity and

adsorption rate of each component decreased compared to the single system. The results indicated that the cationic competitors

influenced the Pb^{2+} adsorption, or vice versa, depending on the amount of charge and adsorption affinity.

Key words: the binary pollutant; adsorption competition; silica gels; kinetics adsorption

INTRODUCTION

Water pollution caused by adverse industrial activities has been becoming a serious threat. Concern on access to pure water for human consumption and agricultural use, and risk of jeopardizing aquatic life have jointly necessitated an escalated finding for water remediation (Bhat et al., 2015; Kushwaha et al., 2020). Numerous techniques and approaches such as membrane separation, ion exchange, precipitation, flocculation and coagulation, bio- and photo- degradation, adsorption have been engaged for the removal of pollutant from water (Tamez et al., 2016; Liang et al., 2016). Among these technologies, the key and foremost method with property of greenness, cost effectiveness, efficiency, and convenient ways of generating adsorbent is the adsorption, which emphasizes the adherence of pollutant (atoms, ions, or molecules) onto the surface of adsorbent (Karaca et al., 2018).

Pollutants such as Pb, Cu, Cr and dye effluents are largely produced from industrial activities (Kumar et al., 2019). A significant amount of these pollutants is noticeable and undesirable, and their concentration beyond permissible limit causes serious threat to the human and aquatic lives (Kavand et al., 2020). The United States Environmental Protection Agency (U.S. EPA) regulates that the permissible pollutants in water systems were 0.015 $mg.L^{-1}$ and 1.3 $mg.L^{-1}$ for Pb^{2+} and Cu^{2+}, respectively (Chen et al., 2019). Besides, low concentration of dyes ($C < 1$ $mg.L^{-1}$) caused a detrimental effect on aquatic ecosystems and human health (Salleh et al., 2011). However, the presence of the multicomponent pollutants caused more complications to be removed from the water system (Tamez et al., 2016).

To date, removal of these pollutants has been dominated using adsorbent derived from low-cost

material such as clay, zeolite, bio-sorbent, agricultural and industrial waste. Agricultural waste

is a potential adsorbent due to shorter process time and re-usability, but the usage of industrial waste such as coal fly ash is also a good option as an adsorbent. Recently, there are considerable attention in the use of coal fly ash as adsorbent which composed of SiO_2 64.97 %; Al_2O_3 26.64 %; and Fe_2O_3 5.69 % that are responsible for the adsorption site (Adak et al., 2014). The adsorption activity of coal fly ash due to its composition has proven effective for removal of pollutants (Gollakota et al., 2019). The adsorption capacity of heavy metals such as Pb and Cu using fly ash can reach consecutively 5.1 $mg.g^{-1}$ and 4.4 $mg.g^{-1}$ (Alinnor, 2007) while the removal methylene blue reach 7 $mg.g^{-1}$ (higher compared to heavy metals) (Wang et al., 2008). Other than that, conversion of fly ash to SG was one of the strategies to increase the adsorption capacity. In the previous studies, the adsorption capacity of methylene blue using silica gel increased by 27.64% compared to fly ash (Sulistiyo et al., 2017).

Herein, we investigate the adsorption of Pb(II) with heavy metal competitors Cu(II) (Pb-Cu), or cationic dye methylene blue (Pb- MB) using SG prepared from coal fly ash. Because of the reality viewpoint, adsorption processes in single and binary batch systems using an artificial solution were studied. The choice of SG among oxides in coal fly ash is therefore governed by the fact that it possesses a large number of silanol groups and well-defined surface properties which enables for the cationic pollutants (Goscianska et al., 2013). The study also focused on the interaction between silica and adsorbate, and kinetic of the single and binary systems.

MATERIALS AND METHODS

Coal Fly Ash Sample and Chemicals

Coal fly ash was collected as combustion waste from PT. POMI Paiton, Probolinggo, East Java, Indonesia. H_2SO_4 (95%, Sigma Aldrich), HCl (37%, Sigma Aldrich), NaOH (99%, Sigma

Aldrich), $Pb(NO_3)_2$ (99%, Sigma Aldrich), $Cu(NO_3)_2.3H_2O$ (99%, Sigma Aldrich) and methylene blue (95%, Sigma Aldrich) were used as received from the manufacturers.

Preparation of Silica Gel

SG was extracted and isolated from fly ash in the same manner as described Kalapathy et al., (2002). The fly ash was washed, dried in an oven prior to the synthesis. NaOH (3 M) was added to the cleaned fly ash and the mixture was refluxed, operated at 90 °C for 2 h. The mixture was then filtered to remove the solid residue. To the filtrate HCl (1 M) was added and stirred until pH 7 was reached and allow standing for 18 hours. The gel formed was collected, washed, and dried in oven at 60 °C overnight. The product was calcined at 550 °C for 4 hours to remove the water content and impurities.

Characterisation of silica gels

SG was characterized by powder X-ray diffraction PANanalytical X'pert using Cu-Kα radiation (40kV, 40mA) in λ 1,5404 Å with 2θ = 5-50°. The surface morphology was examined by SEM FEI Inspect-S50 with a magnification of 80.000 times. Surface area and pore size were determined using Quantachrome Instrument NOVA 1200e. Furthermore, the SG functional group before and after adsorption were characterized by FTIR Shimadzu Prestige 21 at wavenumber 400 – 4000 cm^{-1}.

Adsorption Experiment (Single & Binary Pollutants)

The adsorption of single and binary pollutants was carried out in different pH values and time in a batch system using 0.1 g of the adsorbent and 25 mL of adsorbates at room temperature. The mixture was stirred under constant agitation velocity of 100 rpm at different reaction time. The residual concentrations of heavy metals were determined using Atomic Adsorption Spectrophotometer (Buck Scientific 205) and dye concentrations were evaluated by a UV- Visible spectrophotometer (Spectronic 20 Genesys, Thermo Fischer Scientific). Simultaneous adsorption was also carried out to investigate the Pb adsorption mechanism on other existing pollutants such as dyes (Pb-MB) or other heavy metals (Pb-Cu). Measurements

of residual concentrations were carried out as described in single pollutant experiment. The similar conditions and initial

concentration of the binary mixed adsorbates of about 200 mg.L^{-1}.

The amount of adsorbates which adsorbed on SG was calculated by the following formula in eq. (1).

$$q = \frac{(C_0 - C_e).V}{W} \quad (1)$$

Where q is the adsorption capacity at equilibrium of adsorbate per unit mass of adsorbent (mg.g^{-1}), C_0 and C_e are consecutively the initial and equilibrium concentration (mg.L^{-1}) of the adsorbate, V is the volume of adsorbate solution (L), and W is the mass of adsorbent (g).

Kinetics studies of the adsorption

Kinetics of adsorption was not only to evaluate the efficiency of adsorption but also to examine the mechanism of the adsorption process (Ozdes et al., 2011). Some of the kinetics adsorption models that are commonly used are pseudo-first order, pseudo-second order, interparticle diffusion, and Elovich models following Table 1.

Table 1. The linierity formula of kinetic adsorption models

Kinetic Models	**Formula**
Pseudo-first-order by Lagergren Models	$\ln(q_e - q_t) = lnq_e - k_1 t$
Pseudo-second-order by Ho and McKay	$\frac{t}{q_t} = \frac{1}{k_2 q_e} + \frac{t}{q_e}$
Intra-particle Diffusion	$q_t = k_t t^{1/2} + C$
Elovich Equation	$q_t = \frac{1}{\beta \ln(\alpha\beta)} + \frac{1}{\beta \ln t}$

RESULTS AND DISCUSSION

Characterization of Silica Gels

The amorphous structure of SG was shown by a broad peak at 2θ around 25° from diffractogram x-ray (Fig.1.a), and irregular spherical shape from the SEM image (Fig.1.c). The successful

removal of metal impurities from fly ash can be seen from the high percentage of Si and O elements (Fig.1.d). The N_2 gas adsorption-desorption isotherm profile of the SG is classified as type IV (Fig.1.b), with a hysteresis loop from the pore capillary condensation with the surface area, pore size, and pore volume of 143.55 $mg.g^{-1}$, 1.9 nm, and 0.279 $cm^3.g^{-1}$, respectively.

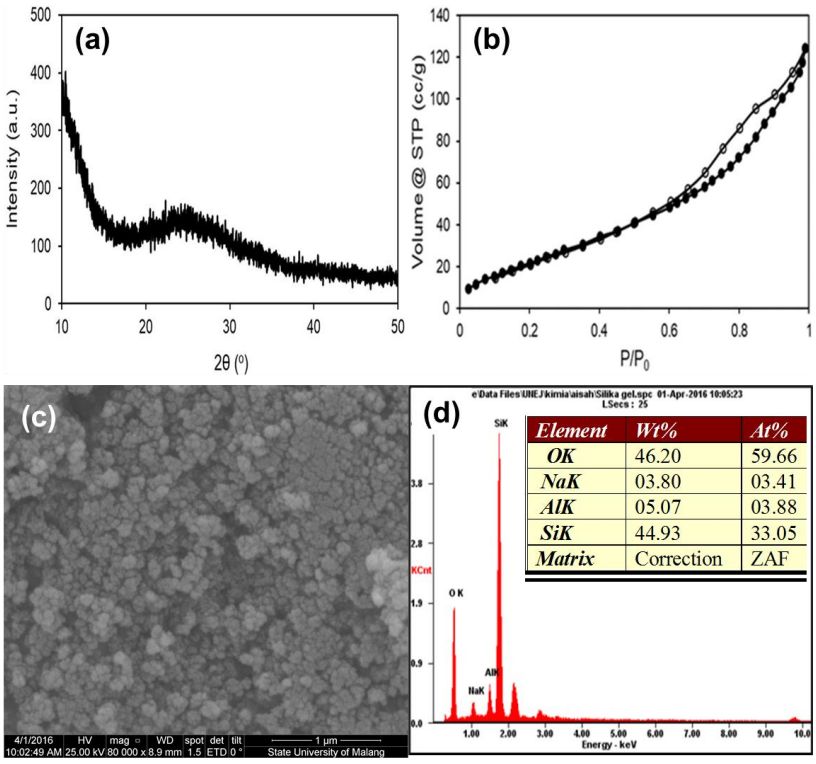

Figure 1 Characterization of SG from coal fly ash using: Diffractogram x-ray (a), Isotherm ads-des of N_2 (b), SEM Image (c), EDX elemental analysis (d)

The FTIR analysis identified the shifting functional groups at SG before and after adsorption. The FTIR spectra (Fig. 2) show the stretching and bending of a hydroxyl group (–OH) from the silanol group (Si-OH) at the peaks of 1635.69 cm^{-1} and 3448.84 cm^{-1}, respectively,

while the peaks were at 461.00; 715.61; and 1057.03 cm^{-1} were the bending, stretching symmetry, and stretching asymmetry of Si-O-Si that showed the siloxane. Fig.2. b-f indicates that the adsorption process affects the silanol group as an active site of silica as illustrated by the reduction in peak area at 1635.69 and 3448.84 cm^{-1}. Cationic exchange of silanol in the silica surface is the

most relevant, although not the sole mechanism that causes these decreasing peaks (Kutzner et al., 2014). Hernández-Montoya and co-worker also reported that the cation exchange as the relevant

interaction models for adsorption using the silanol group on the surface of materials that exhibited in scheme 2 and 3 (Hernández-Montoya et al., 2013).

Heavy metals: $Si\text{-}OH + M^{2+} \rightarrow (Si\text{-}O)_2\text{-}M + 2H^+$ (2)

Cationic dye: $Si\text{-}OH + C\text{-}N^+ \rightarrow Si\text{-}O\text{-}N\text{-}C + H^+$ (3)

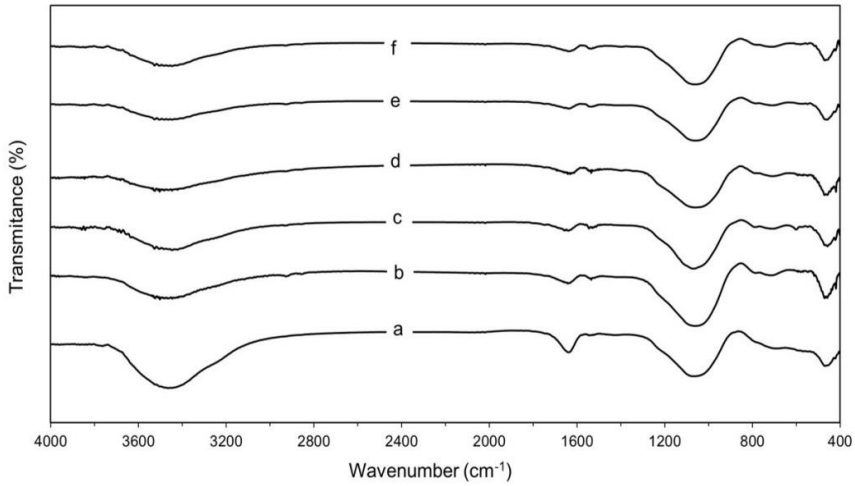

Figure 2 FTIR Spectra of: SiO_2 (a), SiO_2/Pb (b), SiO_2/Cu (c), SiO_2/MB (d), SiO_2/Pb-MB (e), SiO_2/Pb-Cu (f).

Effect of pH on the adsorption capacity

The different adsorption behaviors for each Pb, Cu, and Methylene blue through different pH values 1 - 10 (Fig. 3) indicates the dissociation process of the functional groups and surface charges of SG. The pH affects the surface charge of the adsorbent, the degree of ionization of the adsorbate molecules, and the extent of dissociation of the functional groups on the active

sites of the adsorbent (Silva et al., 2012). The surface charge of the SG was changed from protonated (Si-OH) and deprotonated (Si-O-) across different pH solutions.

SG adsorbents have species for silanol groups on its surface, where their presence with Si-OH and Si-O- are in pH < 6 while Si-O- alone is in pH > 6 (Adam et al. (2013); Wu et al., 2013). The adsorption process of the Si-OH is a combination mechanism between the electrostatic interaction with the cationic absorbate and cationic exchange, surface complexation phenomena, or van der Waals effects (Valdés et al., 2012). The negative charges on the surface of silica have

electrochemical interaction with cationic molecules of the adsorbate (Huang et al., 2011). Moreover, pH also affects metal species in the solution (Niu et al., 2013).

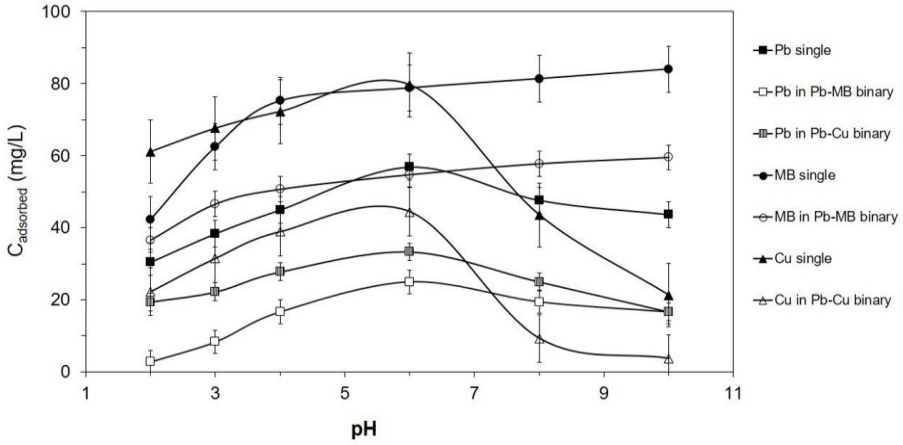

Figure 3 The Models of adsorption in various pH systems Pb^{2+} with the competitor Methylene Blue and Cu^{2+} in single and binary systems by SG

Adsorption capacity of Pb in a single solution using the SG increased from pH 2 to 6, where the gradual increase of the negative charges of SG surface increases the Pb ion interaction on its surface. However, the adsorption capacity decreases with the increase of pH (pH > 6) because of the decreasing electrostatic interaction between $Si\text{-}O^-$ and Pb^{2+} due to the more concentration of $Pb(OH)^+$ and $Pb(OH)_2$, though $Pb(OH)^+$ can interact with $Si\text{-}O^-$ species through hydrogen bonding (Papandreou et al., 2011). In this study, the highest Pb adsorbed on SG was 56.878

$mg.L^{-1}$ at the optimum pH of 6 and it is in good agreement with the finding of Al-Zboon et al. (2011).

The effect of pH was also investigated for adsorption of MB and Cu as competitors in the single system. Similar pattern with that of Pb was observed in Cu^{2+} with higher adsorption capacity of 79.63 $mg.L^{-1}$. Compared to Pb, MB achieved the optimum adsorption capacity in pH 10 of about 84.03 $mg.L^{-1}$. However, MB species were in H_2MB^+ in acid and MB^+ in the basic condition. The high concentration of positive charge from MB+ increases the interaction with $Si\text{-}O^-$.

In the binary systems, the adsorption capacity of Pb^{2+} decreased by 56.05% and 41.40% in the presence of MB and Cu^{2+}, respectively. Similarly, MB and Cu^{2+} were also reduced consecutively by 29.12% and 44.19%. The competitive interaction occurs in the SG surface. The adsorbed adsorbates in the multicomponent adsorption were on the order of methylene blue, Cu^{2+}, and Pb^{2+} (Ding et al., 2016). Methylene blue with bulky structure is expected to have less adsorption affinity, but the result shows the contrary. Ionization state also contributes to the chemisorption type of adsorption and in this regard particle size has no significant role (Noroozi and Sorial, 2013). Based on ionization state, methylene blue (+1) experienced less competition to Pb (+2) or Cu (+2) in the interaction with surface $Si\text{-}O^-$. In the similar ionization state of +2 (Pb and Cu), Cu with the stronger reducing capacity has higher affinity to Si-O- that can also displace Pb interaction in the surface (Zhan et al., 2018).

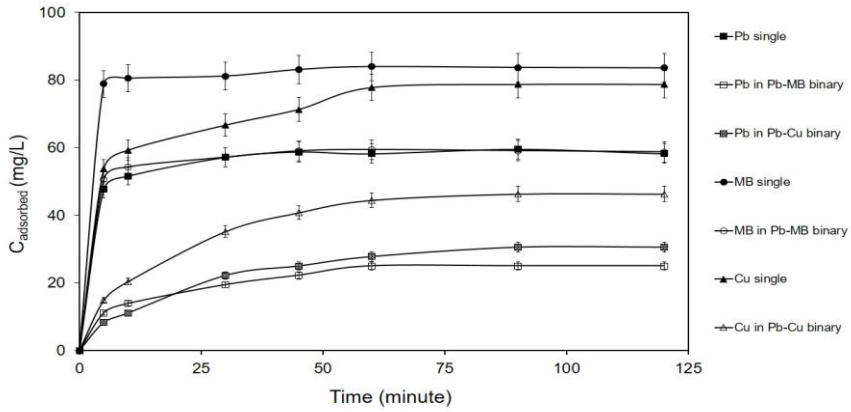

Figure 4 Variation of the time adsorption Pb^{2+} with the competitor Methylene Blue and Cu^{2+} in single and binary systems by SG

Effect of contact time on the adsorption process

The effect of contact time on the adsorption process was carried out in the range of 5-120 min at optimum pH for single and binary adsorption systems. The results showed that adsorption capacity increases with the increased contact time, and the optimum was obtained within 60 min and remained unchanged beyond the optimum time (Fig. 4). In the single adsorption, quick removal of adsorbate occurred in 30 min and slightly increased up to 60 min achieved as the adsorption equilibrium. These conditions describe the adsorption occurs in a two-step mechanism, that is, the rapid adsorption involving external-internal diffusion and slow uptake controlled by intraparticle diffusion until it reaches equilibrium (Michard et al., 1996). Ozdes and co-workers found that fast adsorption has occurred when the metal ions interacted with adsorbent, which more active sites available at the onset of adsorption (Ozdes et al., 2011). The same profile was reported by Huang et al. (2011), the uptake was dramatically rapid for the first 10 min after that, the adsorption was slow up to optimum time of 60 min which highest removal.

Kinetics of adsorption

The adsorption kinetics of single and binary systems onto SG was examined using several kinetic models such as pseudo-first-order, pseudo-second-order, interparticle diffusion, and Elovich equation to determine the adsorption efficiency. The adsorption models followed pseudo-second-order kinetics model with the correlation coefficient (R^2 values) nearly 1 (Table 2). It indicated both the adsorbent and adsorbate affect the adsorption process. The model is consistent with the amount of adsorbed adsorbent calculated (q_e calc.) and experimental data (qe exp.).

Based on model, the adsorption rate of Cu^{2+} is the faster followed by MB and Pb^{2+} in the single system. This is because Cu^{2+} has the smallest atomic size which correlates with the possibility of rapid dispersion on the silica surface. Even though MB has higher molecular weight, its

adsorption rate was faster than of Pb^{2+}. This is because it has +1 molecular charge which in turn make it easier to electrostatically interact with the silica surface charge. Hernández-montoya et al. (2013) also reported that hydroxyl groups have more affinity for the cationic dye than heavy metal. The adsorption rate of the binary system was slower than the single one. MB and Pb^{2+}

occupied different active sites on the silica surface with less competition. However, in Pb and Cu binary-systems, the competition is stronger which correspond to the decrease in the adsorption rate as compared to the single system. The decrease in the binary Pb^{2+} and Cu^{2+} system' adsorption rate was about 10 and 20 times, respectively.

Table 1 Kinetics adsorption of SG on Pb^{2+} with the competitor Methylene Blue and Cu^{2+} in Single and binary systems

Adsorbate		Pb			MB		Cu	
		Single	binary in MB	binary in Cu	single	binary	single	binary
q_e experiment (mg/g)		14.88	4.17	7.64	20.97	14.85	19.68	11.55
Pseudo-first-order	k_1 (min^{-1})	1.5×10^{-3}	8.4×10^{-3}	1.0×10^{-2}	5×10^{-4}	1×10^{-3}	3.2×10^{-3}	8.8×10^{-3}
	q_e ($mg.g^{-1}$)	1.15	2.17	2.58	1.05	1.10	1.35	2.21
	R^2	0.536	0.701	0.688	0.678	0.536	0.774	0.659
Pseudo-second-order	k_2 ($g.mg^{-1}.min^{-1}$)	6.8×10^{-2}	1.5×10^{-2}	5.9×10^{-3}	9.8×10^{-2}	9.4×10^{-2}	1.1×10^{-1}	5.6×10^{-3}
	q_e ($mg.g^{-1}$)	14.82	4.73	8.99	21.09	14.84	20.41	13.11
	R^2	0.999	0.990	0.997	0.999	0.999	0.998	0.998
Interparticle diffusion	k_t ($mg.g^{-1}.min^{-1/2}$)	3.0×10^{-1}	3.4×10^{-1}	6.8×10^{-1}	1.4×10^{-1}	2.2×10^{-1}	7.6×10^{-1}	9.5×10^{-1}
	C	12,00	0.98	1.09	19.60	12.77	12.42	2.63
	R^2	0.728	0.899	0.917	0.823	0.726	0.920	0.886
Elovich Equation	α ($mg.g^{-1}.min^{-1}$)	1.3×10^{5}	8.2×10^{-1}	10.3×10^{-1}	1.3×10^{20}	3.3×10^{7}	229,32	21.1×10^{-1}
	β ($g.mg^{-1}$)	1.10	1.06	0.52	2.47	1.49	0.47	0.37
	R^2	0.891	0.956	0.983	0.975	0.888	0.969	0.975

CONCLUSIONS

In conclusion, SG was successfully synthesized from coal fly ash. with amorphous structure, irregular spherical shapes. As material adsorbent, the Si-OH group of SG interacted with ion Pb^{2+} and its competitors (MB and ion Cu^{2+}) that were exhibited from the decreasing characteristic their peaks in the wavenumber 1635.69 cm^{-1} and 3448.84 cm^{-1}. The maximum uptake of Pb^{2+} and Cu^{2+} was at pH 6 while MB was at pH 10, and the contact time 60 minutes at room temperature. In the single systems, the amount of adsorbed adsorbate followed the order MB > Cu^{2+} > Pb^{2+}. In the binary solution systems, the adsorption capacities of Pb^{2+} decreases in the presence of MB and Cu^{2+}, while each competitor also decreases compared to their single system.

Furthermore, following the pseudo-second-order kinetics models, each adsorbate showed a decrease in the adsorption rate in the Pb-MB and Pb-Cu binary systems. The findings of this study provide an understanding of the adsorption capacity and adsorption rate of each adsorbate in single and binary systems which are influenced by the amount of charge and strength of adsorption affinity with SG.

REFERENCES

Adak D., Sarkar M., & Mandal S. 2014. Effect of nano-silica on strength and durability of fly ash based geopolymer mortar. Constr. Build. Mater. 70, 453–459.

Adam F., Appaturi J.N., Khanam Z., Thankappan R., & Nawi M.A.M. 2013. Utilization of tin and titanium incorporated rice husk silica nanocomposite as photocatalyst and adsorbent for the removal of methylene blue in aqueous medium. Appl. Surf. Sci. 264: 718–726.

Alinnor I.J. 2007. Adsorption of heavy metal ions from aqueous solution by fly ash. Fuel. 86:853–857.

Al-Zboon K., Al-Harahsheh M.S., & Hani F.B. 2011. Fly ash-based geopolymer for Pb removal from aqueous solution. J. Haz. Mater. 188: 414–421.

Bhat A., Megeri G.B., Thomas C., Bhargava H., Jeevitha C., Chandrashekar S., & Madhu

G.M. 2015. Adsorption and optimization studies of lead from aqueous solution using γ-Alumina. J. Env. Chem. Eng. 3: 30–39.

Chen C., Chen Q., Kang J., Shen J., Wang B., Guo F., & Chen Z. 2019. Hydrophilic triazine-based dendron for copper and lead adsorption in aqueous systems: Performance and mechanism. J. of Mol. Liquids. 298: 112031.

Ding G., Wang B., Chen L., & Zhao S. 2016. Simultaneous adsorption of methyl red and methylene blue onto biochar and an equilibrium modeling at high concentration. Chemosphere. 163: 283–289.

Gollakota A.R.K., Volli V., & Shu C.M. 2019. Progressive utilisation prospects of coal fly ash: A review. Sci. Total Env. 672: 951–989.

Goscianska J., Olejnik A., & Pietrzak R. 2013. Adsorption of L-phenylalanine onto mesoporous silica. Mater. Chem. and Phys. 142: 586-593.

Hashemian S., Sadeghi B., & Mangeli M. 2015. Hydrothermal synthesis of nano cavities of Al-MCF for adsorption of indigo carmine from aqueous solution. J. Ind. Eng. Chem. 21: 423–427.

Hernández-Montoya V., Pérez-Cruz M.A., Mendoza-Castillo D.I., Moreno-Virgen M.R., & Bonilla-Petriciolet A. 2013. Competitive adsorption of dyes and heavy metals on zeolitic structures. J. Env. Manag. 116: 213–221.

Huang C.H., Chang K.P., Ou H.D., Chiang Y.C., & Wang C.F. 2011. Adsorption of cationic dyes onto mesoporous silica. Microporous and Mesoporous Materials. 141: 102–109.

Kalapathy U., Proctor A., & Shultz J. 2002. An improved method for production of silica from rice hull ash. Bioresource Technology. 85: 285–289.

Karaca H., Altıntığ E., Türker D., & Teker M. 2018. An evaluation of coal fly ash as an adsorbent for the removal of methylene blue from aqueous solutions: kinetic and thermodynamic studies. J. Dis. Sci. Tech. 39: 1800–1807.

Kavand M., Eslami P., & Razeh L. 2020. The adsorption of cadmium and lead ions from the synthesis wastewater with the activated carbon: Optimization of the single and binary systems. J. Water Proc. Eng. 34: 101151.

Kumar G.V.S.R.P., Malla K.A., Yerra B., & Rao K.S. 2019. Removal of Cu(II) using three low-cost adsorbents and prediction of adsorption using artificial neural networks. Applied Water Sci. 9: 1–9.

Kushwaha A., Rani R., & Patra J.K. 2020. Adsorption kinetics and molecular interactions of

lead [Pb(II)] with natural clay and humic acid. Int. J. Env. Sci. Tech. 17: 1325–1336.

Kutzner S., Schaffer M., Bornick H., Licha T., & Worch E. 2014. Sorption of the organic cation metoprolol on silica gel from its aqueous solution considering the competition of inorganic cations. Water Research. 54: 273–283.

Liang S., Ye N., Hu Y., Shi Y., Zhang W., Yu W., Wu X., & Yang J. 2016. Lead adsorption from aqueous solutions by a granular adsorbent prepared from phoenix tree leaves. RSC Advance. 6: 25393–25400.

Michard P., Guibal E., Vincent T., & Le Cloirec P. 1996. Sorption and desorption of uranyl ions by silica gel: pH, particle size and porosity effects. Microporous Materials. 5: 309–324.

Niu Y., Qu R., Sun C., Wang C., Chen H., Ji C., Zhang Y., Shao X., & Bu F. 2013. Adsorption of Pb(II) from aqueous solution by silica-gel supported hyperbranched polyamidoamine dendrimers. J. Haz. Mater. 244–245: 276–286.

Noroozi B., & Sorial G.A. 2013. Applicable models for multi-component adsorption of dyes: A review. J. Env. Sci. 25: 419–429.

Ozdes D., Duran C., & Senturk H.B. 2011. Adsorptive removal of Cd(II) and Pb(II) ions from

aqueous solutions by using Turkish illitic clay. J. Env. Manag. 92, 3082–3090.

Papandreou A.D., Stournaras C.J., Panias D., & Paspaliaris I. 2011. Adsorption of Pb(II), Zn(II) and Cr(III) on coal fly ash porous pellets. Minerals Engineering. 24, 1495–1501.

Salleh M.A.M., Mahmoud D.K., Karim W.A.W.A.K., & Idris A. 2011. Cationic and anionic dye adsorption by agricultural solid wastes: a comprehensive review. Desalination. 280: 1–13.

Sulistiyo Y.A., Andriana N., Piluharto B., & Zulfikar Z. 2017. Silica Gels from Coal Fly Ash as Methylene Blue Adsorbent: Isotherm and Kinetic Studies. Bull. Chem. React. Eng. & Catal. 12: 263.

Tamez C., Hernandez R., & Parsons J.G. 2016. Removal of Cu (II) and Pb (II) from aqueous

solution using engineered iron oxide nanoparticles. Microchemical Journal. 125: 97–104.

Valdés H., Tardón R.F., & Zaror C.A. 2012. Role of surface hydroxyl groups of acid-treated natural zeolite on the heterogeneous catalytic ozonation of methylene blue contaminated waters. Chemical Engineering Journal. 211–212: 388–395.

Wang S., Ma Q., & Zhu Z.H. 2008. Characteristics of coal fly ash and adsorption application. Fuel. 87: 3469–3473.

Wu Y., Cao J., Yilihan P., Jin Y., Wen Y., & Zhou J. 2013. Adsorption of anionic and cationic dyes from single and binary systems by industrial waste lead–zinc mine tailings. RSC Advance. 3: 10745.

Yao Z.T., Ji X.S., Sarker P.K., Tang J.H., Ge L.Q., Xia M.S., & Xi Y.Q. 2015. A comprehensive review on the applications of coal fly ash. Earth-Science Reviews. 141: 105–121.

Zhan W., Xu C., Qian G., Huang G., Tang X., & Lin B. 2018. Adsorption of Cu(II), Zn(II), and Pb(II) from aqueous single and binary metal solutions by regenerated cellulose and sodium alginate chemically modified with polyethyleneimine. RSC Advance. 8: 18723–18733.